J Solid State Eletrochem (2004) 8: 398–402
DOI 10.1007/s10008-003-0476-7

ORIGINAL PAPER

M. Strawski · M. L. Donten · M. Donten
M. Szklarczyk

Microscopic observation of the crystalline form of poly(*o*-methoxyaniline) on a membrane electrode

Received: 16 July 2003 / Accepted: 4 November 2003 / Published online: 24 January 2004

Abstract We describe electrochemical and microscopic (SEM) studies on the electrochemical polymerization of poly(*o*-methoxyaniline). The crystalline form of the polymer was obtained. The poly(*o*-methoxyaniline) crystals are formed on a membrane electrode from an acidic solution of the monomer. It is suggested that the pores of the membrane work as nuclear crystallization points.

Keywords Crystal structure · Crystalline polymer · Membrane electrode · Poly(*o*-methoxyaniline) · Scanning electron microscopy

Introduction

Conjugated polymers, in particular the more than a century-old polyaniline (PANI) [1, 2, 3] and its derivatives, have attracted significant attention thanks to the straightforward methods of their preparation (e.g. [4, 5, 6]) and the good stability of the conductive form in aqueous solution [7, 8], as well as multiple potential applications [9, 10]. Considering the large number of papers devoted to research either on redox processes or physicochemical properties and the polymerization mechanism of conducting polymers, there have been relatively fewer studies on the morphology and type of the crystalline form of the synthesized polymers, even though it is known that polymer properties are dependent on the crystalline structure and morphology [11, 12, 13, 14, 15, 16, 17]. Two forms of morphology are considered: globular and fibrillar.

In the quest for improved performance, better processable newer compounds of different crystallographic structure have been synthesized. The modification of the polymeric structure can produce materials with new physical characteristics. The crystalline structures of polyacetylene, polyethylene, and polythiophene have already been observed and widely discussed ([16] and references therein). The first observations of crystallinity in some chemically grown polyaniline samples were reported by Wang et al. [18] and Moon et al. [19]. The different structural models, dependent on the oxidation state and doping level, have been proposed on the basis of X-ray studies [20, 21].

A report on the crystallinity of PANI samples grown under electrochemical conditions has recently been published [22]. It was observed by scanning electron microscopy (SEM) and X-ray diffraction techniques (XRD). The authors of the article [22] attributed the catalytic activity of PANI to its crystalline form, pointing out that crystalline PANI is more active towards certain reactions than amorphous PANI. The thickness of the PANI crystalline layer was reported to be about 0.08 μm.

In this paper we report the results of the electrochemical polymerization of *o*-methoxyaniline on membrane electrodes. Currently, membrane electrodes are widely used in electrochemistry because they work as a template for different nano- and microstructure syntheses. Generally, the processes taking place on the top of the membrane during the electrosynthesis are not studied. Our studies were focused on the polymerization process taking place on the top of a membrane. To prove the presence and to characterize the polymeric film, we have employed SEM and X-ray energy dispersive spectroscopy (EDS) techniques.

Contribution to the 3rd Baltic Conference on Electrochemistry, Gdansk-Sobieszewo, Poland, 23–26 April 2003

Dedicated to the memory of Harry B. Mark, Jr. (28 February 1934–3 March 2003)

M. Strawski · M. L. Donten · M. Donten · M. Szklarczyk (✉)
Laboratory of Electrochemistry, Department of Chemistry,
Warsaw University, ul. Pasteura 1, 02-093 Warsaw, Poland
E-mail: szklarcz@chem.uw.edu.pl
Tel.: +48-22-8220211
Fax: +48-22-8225996

Experimental

Electrodes

The working electrodes were made of Nucleopore track-etched polycarbonate membranes (Whatman, USA). The backside of the membrane (the one opposite to the solution) was covered with platinum by the sputtering technique in order to secure an ohmic contact. The membrane pore diameters were 100 nm and 400 nm. The membrane electrodes were washed with acetone and then with Millipore water before being placed in the electrochemical cell. For comparison, a polished Pt disk was also used as a working electrode in some experiments. The working surface of the Pt disk was polished with alumina down to 1 μm. After polishing, the Pt electrode was placed in an ultrasonic bath and washed with Millipore water to remove all polishing residues.

The counter electrodes were made of Pt/Pt gauze or wire and the electrode potential was measured against an Ag/AgCl electrode placed in saturated KCl solution.

Solutions

All solutions were prepared from Millipore-Q water. The supporting electrolyte solution, 1 M $HClO_4$, was prepared from concentrated reagent-grade perchloric acid and stored under an argon atmosphere in a glass flask; the *o*-methoxyaniline monomer was obtained from Aldrich and was distilled prior to use. The transfer of the supporting electrolyte from the storage flask to the electrochemical cell was done under an argon atmosphere. All experiments were carried out at ambient temperature, 22 ± 2 °C.

Equipment and experimental procedures

A three-electrode cell was used in all experiments. The current–voltage behavior was monitored with a programmed potentiostat (EG&G 263A, USA).

The SEM images were taken with a LEO 435 VP microscope (Germany). The device was working with a low sample current to give the highest possible resolution and detailed structure imaging. Under such conditions the effect of charge-up was diminished. The chamber pressure was 10^{-6} Torr and pictures were registered for 7 keV or 15 keV electron beam energy to obtain the best quality images. Before placing in a vacuum the samples were washed with Millipore water and then dried.

Elemental analysis measurements were carried out with a multichannel EDS device (Röntec, model M1, Germany).

Results and discussion

Electrochemical studies

The current–potential (*i–E*) dependences for a Pt disk electrode over a wide potential range (−0.20 to 1.20 V, solid line) and over a narrow one (0–1.0 V, dotted line), as well as for a membrane electrode over the narrow potential range (dashed line), placed in the supporting electrolyte solution are shown in Fig. 1. The application of a narrow scanning potential range for membrane electrodes was necessary in order to avoid, on the one hand, the splitting of the sputtered platinum layer from the membrane because of hydrogen and oxygen evolution, and, on the other, in order to avoid electrochemical degradation of the electrodeposited poly(*o*-methoxyaniline) (POMA) layer [23].

The first, fourth and steady-state *i–E* curves registered for the Pt disk electrode and for the membrane electrode after addition of the *o*-methoxyaniline monomer to the electrochemical cell are shown in Fig. 2 and Fig. 3, respectively. The steady state *i–E* curves were reached after about 1 h cycling at a sweep rate of 50 mV s^{-1}. The slight potential shift of the anodic and cathodic peaks for the platinum disk electrode and membrane electrode, especially for the steady-state dependence, can be noted. We link these differences to the different diffusion conditions comparing the Pt disk electrode with the membrane electrode. The electrochemical results presented show that the polymerization process takes place at the membrane electrode analo-

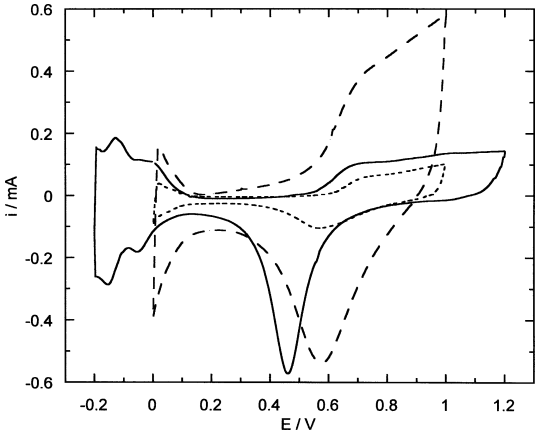

Fig. 1 Cyclic voltammograms of a Pt disk electrode over a wide potential range (*solid line*) and over a narrow potential range for a Pt disk electrode and a membrane electrode (*dotted line* and *dashed line*, respectively) in 1 M $HClO_4$ solution in the absence of monomer in the bulk of solution. Sweep rate: 50 mV s^{-1}

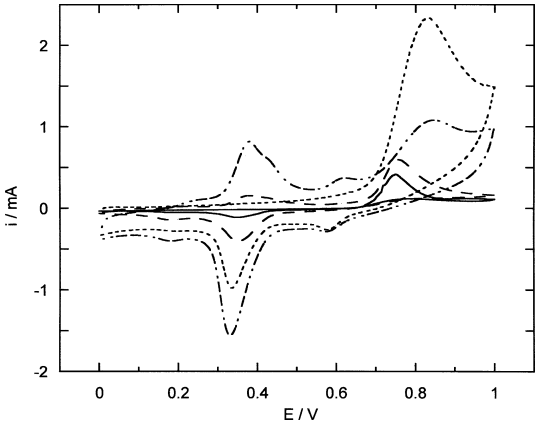

Fig. 2 Cyclic voltammograms of a Pt disk electrode and a membrane electrode in 1 M $HClO_4$ solution after addition of the *o*-methoxyaniline monomer ($c = 0.03$ M) to the bulk of solution. The first and fourth curves are presented for the Pt electrode (*solid line* and *dashed lines*, respectively) and for the membrane electrode (*dotted line* and *dashed-dotted line*, respectively). Sweep rate: 50 mV s^{-1} and 5 mV s^{-1} for the membrane and Pt disk electrodes, respectively

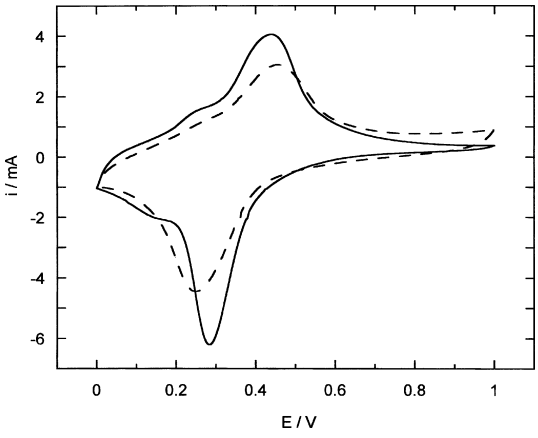

Fig. 3 Steady-state cyclic voltammograms of the Pt electrode and the membrane electrode covered with POMA (*solid line* and *dashed line*, respectively). Monomer concentration: 0.03 M in 1 M $HClO_4$ solution. Sweep rate: 50 mV s^{-1}

gously to the polymerization process occurring at the Pt electrode. It is worth noticing that the oxidation peak at ca. 0.6 V, showing the oxidation of the benzoquinone species formed in the hydrolysis process, is more distinct at the membrane electrode (Fig. 2). The replacement of the monomer-containing solution for the monomer-free solution did not influence the shape of the steady-state *i*–*E* dependences. From this observation it seems apparent that under the studied conditions a stable layer of POMA was attained. Obtaining a stable layer of polymeric deposit allowed safe transfer of the samples to the microscopy vacuum chamber.

SEM and EDS studies

The membrane electrode surface after an electrochemical experiment was carefully washed with Millipore water, then dried and transferred into the microscope vacuum chamber. Typical images registered for membrane electrodes with 100 nm and 400 nm pore diameter are shown in Fig. 4a and Fig. 4b, respectively. The pores are easily distinguishable and their diameter is about that specified by the producer. The whiter wafts, which are in particular visible for membranes with 400 nm diameter pores, are the result of a local charge-up effect occurring because of the low conductivity of the membrane. Such an effect was not observed when the membranes were covered with a thin gold layer, which is the usual way to increase the conductivity of SEM objects. The microscopic images presented were taken for the membranes not covered with the gold layer because we did not want to introduce into the monitored system any species other than those obtained in the electrochemical cell.

The morphology of the membrane electrode after the polymerization process was shown in Fig. 5. In Fig. 5a a large-area picture of a 100-nm pore diameter membrane is presented. The surface consists of many easily distin-

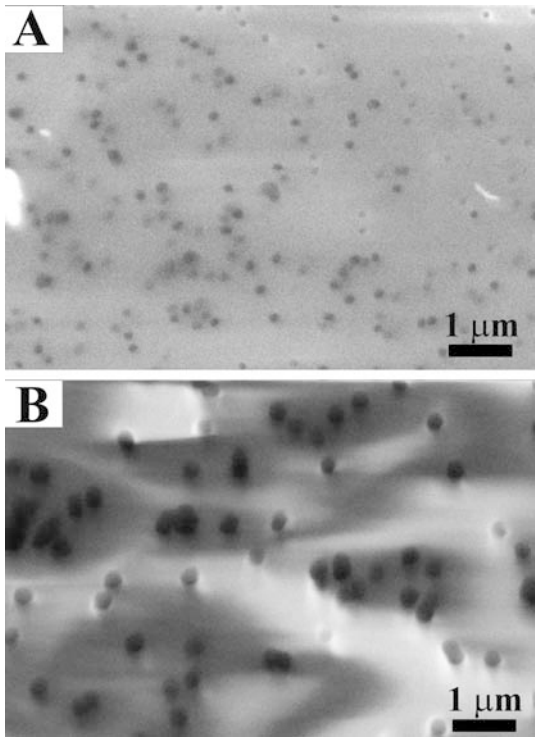

Fig. 4 SEM images of the membrane electrode surface: **A** membrane with 100 nm pores; **B** membrane with 400 nm pores

guishable solid structures of different length, ranging from ca. 0.2 μm to 2 μm. The shape of the observed surface structures differs from that observed for polymers deposited on metallic electrodes (e.g. [24, 25]). Moving the microscope sample holder in the *X* and *Y* directions proved that the surface polymeric structures could be found at any part of the surface. To identify the nature of monitored structures it is necessary to consider their possible origin. They could be formed either in some salt crystallization process, or during evaporation of platinum on the backside of the membrane if Pt were to come through the pores onto the working side of the membrane. Then they could be formed from the polymer during the electropolymerization process. The first considered source of the surface structures (salt crystallization) is the least likely to occur, firstly because the polymerization process was carried out from an acidic solution, and, secondly, because the membrane was carefully washed with water before being placed in the microscope chamber. The second source (platinum evaporation) was excluded by EDS analysis, which did not show the presence of platinum on the working surface of the membrane. Similarly, EDS did not show the presence of any metals which could be present in some salts. Under such circumstances it is assumed that the observed surface structures are made only of POMA.

The magnification of the discussed POMA structures is given in Fig. 5b. Under higher magnification the crystalline-like structure of the polymeric structures is easily recognized. The grain boundaries are easily

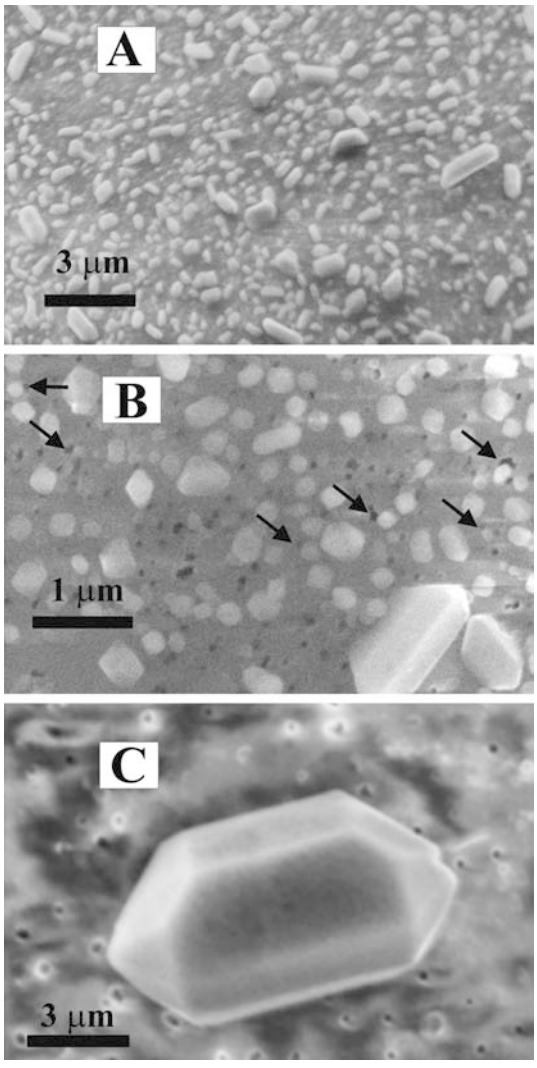

Fig. 5A–C SEM images of the membrane electrode surface taken after the polymerization process was carried out. The pictures **A** and **B** were registered at a different magnification for a membrane with 100 nm pores. The *arrows* point to a few places where the surface structures coming up out of the pores are easily seen. **C** was taken of a membrane with 400 nm pores

distinguishable and visible grain angles are equal to $57 \pm 6°$, $91 \pm 4°$ and $141 \pm 9°$. The crystallographic structures determined by XRD for PANI crystals reported in the literature differ from each other, e.g. for PANI grown chemically the orthorhombic structure was proposed [21], while for thin films of electrochemically grown PANI on a Ni electrode the rectangular structure was proposed [22]. In the case of the results presented in this paper, only a preliminary structure determination can be suggested. This is because at the present stage of our studies the X-ray diffraction and X-ray powder diffraction techniques cannot be applied to crystallographic characterization because of the too small dimensions of the grown crystals and problems in distinguishing the POMA signal from the membrane signal, respectively. On the basis of the determined grain angles, an oblique structure of the grown POMA crystals is the most probable one.

The dimension of the crystallites depends on the pore diameter. The crystals grown on the 400 nm pore diameter membrane electrode were found to be up to 10 μm long (Fig. 5c). A preliminary analysis of the results presented in Fig. 5b suggests that the surface structures start to grow at the membrane pores (cf. pointing arrows in Fig. 5b). Hence, it can be assumed that pores, as the surface discontinuity, work as crystallization nuclei. Our observations indicate that the dimensions of the polymeric crystallites are both pore diameter and time dependent. These observation indicate that the growing of larger crystals than presented in this paper can be achievable; consequently the application of the XRD technique for crystallographic structure determination should also be possible in future.

The images shown in Fig. 5b and Fig. 5c demonstrate that the polymer blocks only part of the pores. The still visible pores are of smaller diameter than those observed before the polymerization process was carried out (cf. Fig. 4a, b and Fig. 5b, c). It is proposed that the diminishing of the pore diameter results from the growth of polymeric tubules along the pore walls.

Conclusions

Membrane electrodes are generally used as a matrix for polymeric tubule synthesis. Studies of the membrane surface after the electropolymerization process have shown that they can also be used for the electrochemical growth of the crystalline form of POMA. Furthermore, the dimensions of synthesized crystallites depend on the membrane pore diameter.

Acknowledgements The authors gratefully acknowledge the support of this work under grant KBN 7T09A 025 20.

References

1. Letherby H (1862) J Chem Soc 15:161
2. Green AG, Woodhead AE (1910) J Chem Soc 97:2388
3. Green AG, Woodhead AE (1912) J Chem Soc 101:1117
4. Mohilner DM, Adams RN, Argersinger WJ (1962) J Am Chem Soc 84:3618
5. MacDiarmid AG, Mu SL, Somasiri NL, Wu W (1985) Mol Cryst Liq Cryst 121:187
6. Gottesfeld S, Redondo A, Feldberg SW (1987) J Electrochem Soc 134:271
7. Huang WS, Humprey BD, MacDiarmid AG (1986) J Chem Soc Faraday Trans 86:2385
8. Yang CY, Cao Y, Smith P, Heeger AJ (1993) Synth Met 53:293
9. Johnstone B (1988) East Econ Rev 17:78
10. Scrosati B (1993) Application of electroactive polymers. Chapman & Hall, New York
11. Deits W, Cukor M, Rubner M (1981) Polym Sci Technol 82:209
12. Chao F, Costa M, Tian C (1995) Synth Met 75:85
13. Łużny W, Trznadel M, Proń A (1996) Synth Met 81:71
14. Skompska M, Szkurat A (2001) Electrochim Acta 47:4007

15. Jiang X, Harima Y, Yamashita K, Tada Y, Ohshita J, Kunai A (2002) Chem Phys Lett 364:616
16. Morton-Blake DA, Corish J (1996) Atomistic simulation investigation of electroactive polymers. In: Lyons MEG (ed) Electroactive polymers electrochemistry, part 2, chap 5. Plenum, New York, pp 1–78
17. Skompska M, Szkurat A, Kowal A, Szklarczyk M (2003) Langmuir 19:2318
18. Wang F, Tang J, Wang L, Zhang H, Mo Z (1988) Mol Cryst Liq Cryst 160:175
19. Moon YB, Cao Y, Smith P, Heeger AJ (1989) Polym Commun 30:196
20. Józefowicz ME, Laversanne R, Javadi HHS, Epstein AJ, Pouget JP, Tang X, MacDiarmid AG (1989) Phys Rev B 39:12958
21. Józefowicz ME, Epstein AJ, Pouget JP, Masters JG, Ray A, Sun Y, Tang X, MacDiarmid AG (1991) Synth Met 41–43:723
22. Rajendra Prasad K, Munichandraiah (2002) Synth Met 130:17
23. Malinauskas A, Holtze R (1998) J Appl Polym Sci 73:287
24. Paul RK, Pillai CKS (2000) Synth Met 114:27
25. Hu C-C, Chen E, Lin J-Y 2002) Synth Met 47:2741